Published by IOP Publishing for Sissa Medialab

Received: *September 30, 2024*
Revised: *December 18, 2024*
Accepted: *January 2, 2025*
Published: *March 26, 2025*

25th International Workshop on Radiation Imaging Detectors
Lisbon, Portugal
30 June – 4 July 2024

Neutron energy measured by Time-of-Flight technique with triggered MiniPIX-Timepix3 detector with Si and SiC sensors

D. Poklop[a,b,*] **C. Granja**[a,c] **P. Alexa**[a] **R. Uhlar**[a] **D. Kuca**[a] **M. Koprda**[c] **D. Hladik**[c] **P. Krist**[b] **and J. Jakubek**[c]

[a] *Department of Physics, VSB-Technical University of Ostrava, 17. listopadu 2172/15, 708 00, Ostrava, Czech Republic*
[b] *Nuclear Physics Institute, Czech Academy of Sciences, Hlavni 130, 250 68, Husinec-Rez, Czech Republic*
[c] *Advacam, U Pergamenky 12, 170 00, Prague 7, Czech Republic*

E-mail: dusan.poklop.st@vsb.cz

Abstract: For fast neutron sources, such as compact neutron generators, it is desirable to have knowledge and ideally directly measure the energy spectrum of the generated neutrons. For neutrons, the produced radiation field, and the neutron energy spectrum, at a specific location from the source, can be altered by the distance to the source and become even significantly distorted by surrounding material — e.g. walls and the floor of the laboratory. To achieve this goal, we make use of the Time-of-Flight (ToF) technique, which has been implemented on the Timepix3 detector operated in highly integrated readout electronics as a miniaturized radiation camera MiniPIX-Timepix3. Equipped with a silicon sensor, the Timepix3 ASIC chip provides fast timing response of individual pixels at the nanosecond level. In this work, we use two Timepix3 detectors with a silicon sensor of thickness 300 µm and a segmented neutron conversion mask, intended for both thermal and fast neutrons and with a 65 µm thick silicon carbide (SiC) sensor. Demonstration and evaluation of the technique are provided by measurements with a compact neutron D-T pulsed generator at VSB-TU Ostrava laboratory which produces mono-energetic 14 MeV neutrons.

Keywords: Instrumentation for neutron sources; Trigger detectors

*Corresponding author.

https://doi.org/10.1088/1748-0221/20/03/C03045

Contents

1 Motivation, aims

For fast neutron sources, such as compact neutron generators, it is important to detect with high discrimination and measure the energy spectrum of the generated neutrons if possible. However, the neutron spectrum can vary significantly depending on the distance from the sources, creating a specific radiation field at a given point. This field can be greatly affected by the surrounding environment, for example the materials that surround the neutron source — such as the walls and floor of the laboratory. These materials can cause scattering, absorption or reflection of neutrons, which can greatly distort the neutron spectrum in different parts of the laboratory. For this purpose, we apply the Time-of-Flight (ToF) technique on the Timepix3 ASIC chip [1, 2].

2 Instrumentation and experimental setup

2.1 Monoenergetic 14 MeV neutrons

We performed measurements on a compact neutron generator MP320 (figure 1a) at the laboratory for neutron activation analysis and gamma spectrometry at VSB-Technical university of Ostrava. This type of generator makes it possible to generate neutrons with a precisely defined energy, which is crucial for experimental studies in the field of neutron detection and measurement. The neutron generator (NG) produces mono-energetic 14 MeV neutrons from deuterium-tritium fusion (D-T reaction) and maximum operational neutron yield is approximately 10^8 neutrons/s [3]. For this experiment we use 100 Hz neutron source frequency with 5% duty factor.

2.2 Triggered Timepix3 detectors with Si and SiC sensors

For this work we use the Timepix3 operated and readout by the miniaturized radiation camera MiniPIX-Timepix3 [4] to which the additional signal trigger-in electronic interface has been newly developed —

see figure 1b. The electronic reduction switches the optocoupler with trigger signal from generator, which then turns on the trigger in the detector. The electronic reduction galvanically separates the input from the output and enables switching of different voltage levels of the input signals (3–24 V). On the detector side, the voltage is taken directly from the detector from the usb port (5 V) and adjusted to the necessary 2.5 V CMOS trigger signal. Neutron generator provides 5 V TTL trigger signal.

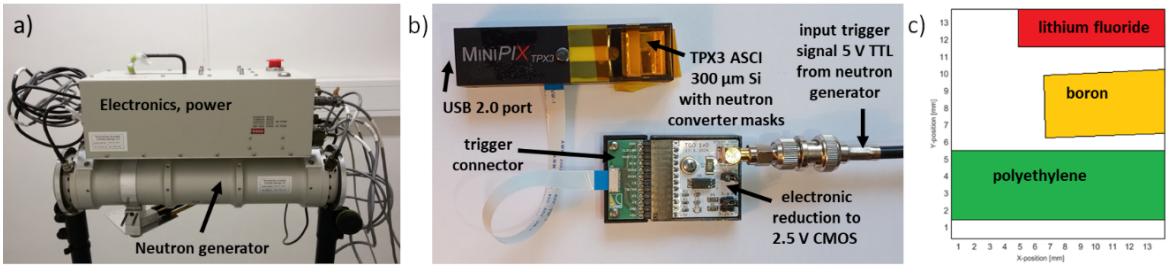

Figure 1. a) D-T neutron generator at VSB-TU Ostrava. b) Radiation camera MiniPIX-Timepix3 with customized trigger electronics. c) Neutron converter mask on the TPX3 Si detector — see text.

The pixel detector with the 300 µm silicon sensor was additionally equipped with a segmented neutron converter mask for thermal and fast neutrons [5]. In figure 1c you can see the type and location of the neutron conversion masks. A lithium fluoride (LiF) thermal neutron converter (red) is in the upper part of the sensor. In the middle region is boron, also a converter for thermal neutrons (yellow). In the lower part there is polyethylene, which serves as a converter for fast neutrons. Each of these regions provides a selective neutron interaction and detection channel, and this channel contributes to the entire detector sensor pixel matrix. In addition, fast and intermediate energy neutrons interact also directly in the detector semiconductor sensor [5].

A novel 65 µm silicon carbide (SiC) sensor without neutron converters has been tested as well [6].

3 Neutron Time-of-Flight technique with Timepix3

Neutron Time-of-Flight (ToF) is an experimental technique used to measure neutron energy based on the time it takes neutrons to travel a known distance. It is an indirect method of determining energy, since neutrons with different energies have different speeds — see table 1. In this way, we can determine not only the energy of individual neutrons, but also the entire energy spectrum of neutrons generated by a specific source. Subsequently, the neutrons travel a known distance (neutron flight path) between the place of their generation and the detector. When neutrons are detected, the time elapsed from their release to impact on the detector is measured (neutron time of flight) [7, 8].

In this experiment, we used the NG generator located in the VSB-TU Ostrava laboratory, the dimensions are shown in figure 2. The neutron generator was set to an operating frequency of 100 Hz with a duty factor of 5% (Pulse period 10 ms and pulse width 0.5 ms). The pixel detector was located 2.7 m from the neutron generator (figure 2). A 6 m coaxial cable was led from the power source of the generators (figure 1a) to the triggering electronics of the detector (figure 1b), which was near the detector. The time delay of the cable and electronics is approximately 260 ns. We set the pixel detector to be triggered by a trigger signal and set the data driven mode with ToA (Time of Arrival) and ToT (Time over Threshold) channels [9].

2025 JINST 20 C03045

Table 1. Time of flight for different neutron energies. The flight path time for the distance 2.7 m is included.

Neutron energy	*Speed of neutron [m/μs]*	*Time of flight [μs]*
14 MeV	51.76	5.21×10^{-2}
1 MeV	13.83	1.95×10^{-1}
100 keV	4.37	6.17×10^{-1}
10 keV	1.38	1.95
1 keV	0.43	6.17
1 eV	1.38×10^{-2}	1.95×10^{2}
25 meV	2.19×10^{-3}	1.23×10^{3}

For a quicker data acquisition, the data was not collected for each trigger signal, but for one trigger followed by many subsequent pulses. The reason for this approach is the detector dead time and the limited neutron detection efficiency of the detectors (for fast neutrons is ~1% for Si sensor, ~0.1% for SiC sensor). When the detector has received the trigger signal, 20 s data acquisition begins. After 20 s of measurement, the detector is waiting for the next trigger signal.

With this setup, we were able to collect 356 files (356 × 20 s = 7120 s of total measured data) for the Si sensor and 14 files (14 × 20 s = 280 s of total measured data) for the SiC sensor.

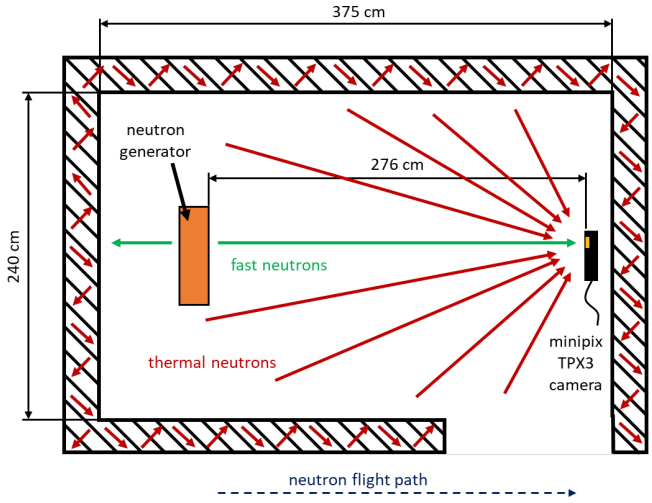

Figure 2. Principle and layout ToF experiment. The pixel detector was placed at 2.7 m from the neutron generator (NG). Fast unmoderated neutrons arrive directly over straight path (green arrows) from the NG. Moderated and thermalized neutrons, interacting and originating in the surrounding materials and walls of the laboratory, arrive to the detector from different directions (red arrows).

4 Results

4.1 Time-, energy- and position-sensitive detection

The radiation field registered by Timepix3 at the detector position in shown in figure 3. Data are shown for a 20 s of continuous measurement after one trigger signal. The data was then offline integrated in consecutive (summed) 10 ms intervals (corresponding to 100 Hz frequency of neutrons source).

2025 JINST 20 C03045

Figure 3a shows the raw data in ToA (Time of Arrival) mode for all measured events. Per-pixel time is displayed on a color scale and has a range of 0–10 ms. In the ToA mode, time is recorded in reverse, i.e. it is information between the registration of the particle and the end of the measurement, not the beginning of the measurement. That is the red scale id for events that were captured first and the blue scale for events that were captured towards the end.

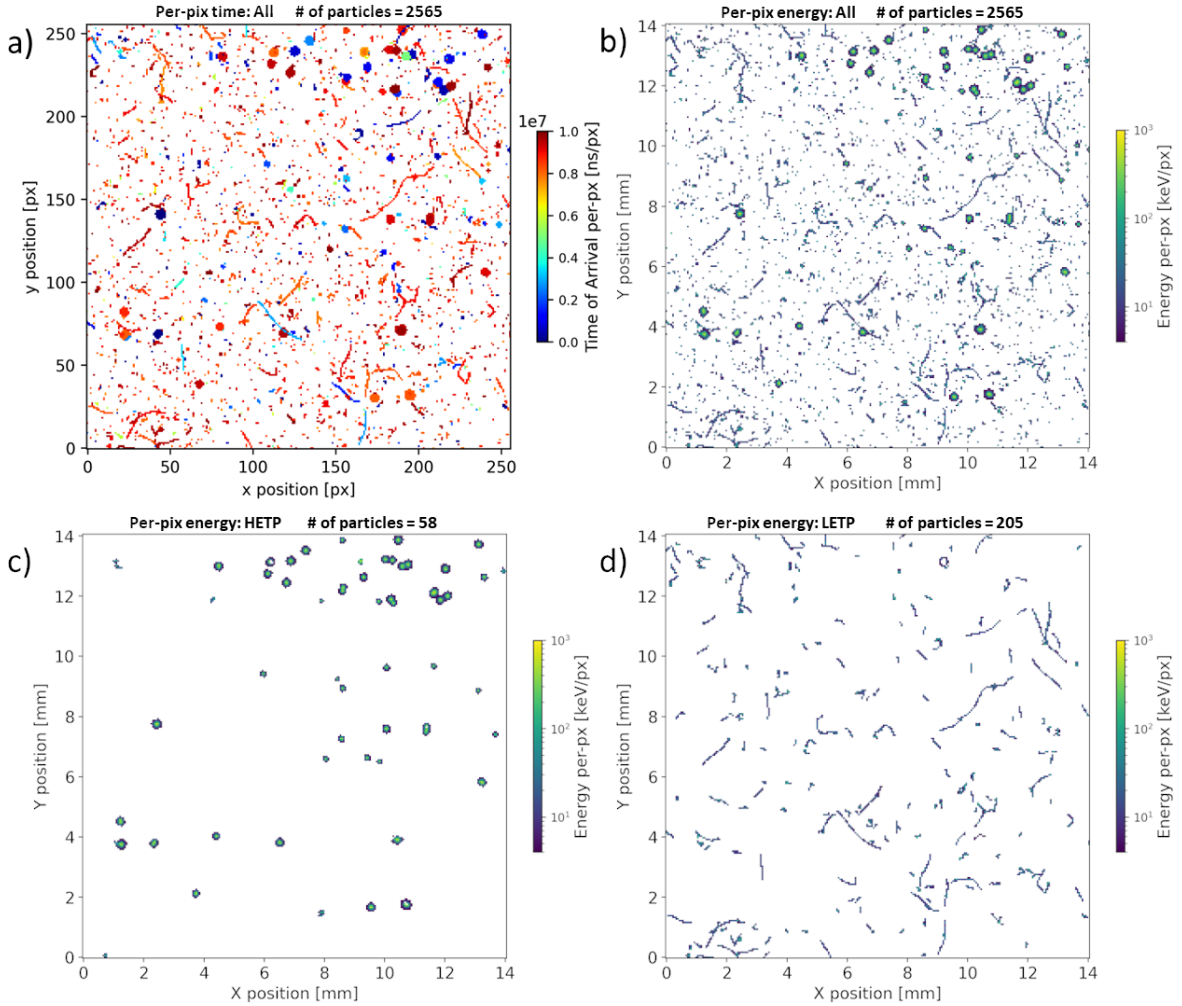

Figure 3. Radiation field visualization a decomposition measured by the Timepix3 Si detector: a) 2D plot of Time of Arrival (ToA), per-px/Time [ns/px] — see color bar, all particles. b) 2D plot of Deposit Energy per-px/E [keV/px] — see color bar, all particles. c) 2D plot of Deposit Energy per-px/E, HETP. d) 2D plot of Deposit Energy per-px/E [keV/px], LEPT.

2D The of deposited energy for all events is show in figure 3b. The per-pixel deposited energy is displayed by the color scale. Figure 3c and figure 3d show radiation field decomposition. Particle-event types on the detector are classified by table 2 which are analyzed by experimental calibrations in well-defined radiation fields using high-resolution pattern recognition analysis of the pixeled tracks [10].

2025 JINST 20 C03045

Table 2. Particle-type resolving power for Timepix3 Si sensor.

Class	*Particle type*	*Radiations*
i	HETP	• protons • ions • neutron
ii	LETP large track	• electrons • protons (non-perpendicular high energy) • minimum ionizing particle • gamma rays low-energy
iii	LETP small track	• X rays • Electrons (perpendicular) • Protons (perpendicular high energy) • Neutrons (intermediate energy)

4.2 Time-of-flight spectra

The results of the experiment are ToF spectra, which are processed for both sensors, the Si sensor shown in figure 4a and the SiC sensor shown in figure 4b.

The resulting ToF spectrum was compiled from all measured data (356 files = 7120 s for the Si sensor and 14 files = 280 s for the SiC sensor). All these data were offline divided in consecutive time segments of 10 ms and then integrated into one spectrum. It was assumed that the NG trigger exhibits the same repetition rate of 100 Hz. For all data, we used the decomposition according to table 2.

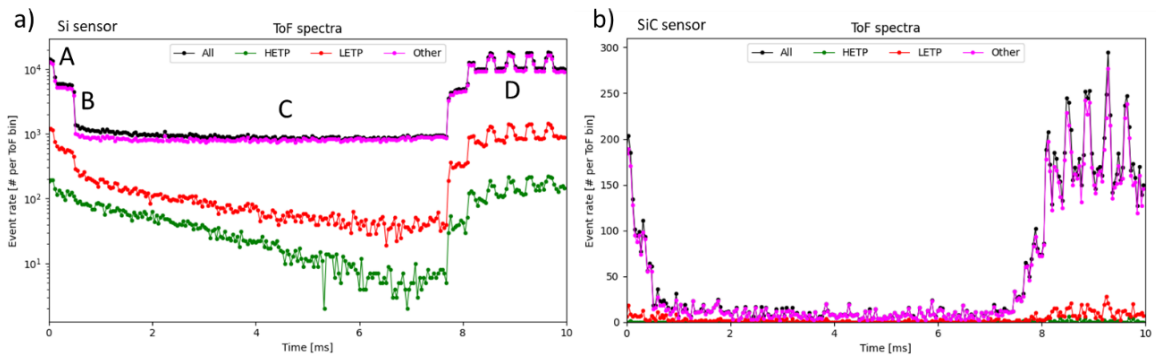

Figure 4. Measured ToF spectra by triggered Timepix3 with a) Si sensor, data shown correspond to total integrated time 356 × 20 s = 7120 s. b) SiC sensor, data shown correspond to total integrated time 14 × 20 s = 280 s. Curves shown for: all particles (black), HETP class i (green), LETP class ii (red) and LETP class iii (purple).

We divided the resulting ToF spectrum into areas A, B, C, D, see figure 4, according to the frequency of occurrence of fast or thermal neutrons. In region A (0–0.13 ms), there is the greatest occurrence of 14 MeV fast neutrons (figure 5a). In region B (0.13–0.51 ms), there are delayed fast neutrons and thermal neutrons from interactions in the walls of the laboratory (figure 5b). In region C (0.51–7.74 ms), there are almost no fast neutrons and thermal neutrons dominate (figure 5c). Both fast and thermal neutrons are found in region D (7.74–10 ms). According to figure 3a in the regions

2025 JINST 20 C03045

of the detector where there is no thermal neutron converter, events corresponding to fast neutrons occur. This suggests that the neutron generator does not maintain a stable frequency of 100 Hz. This must be verified. For further processing, we work with areas A, B and C.

4.3 Time-gated, neutron converter-correlated spatial distributions

Measurement and detailed monitoring of neutrons in terms of particle flux (figure 5, figure 6) allows to estimate the resulting neutron fluxes for a given area of neutron converters and a given area in the ToF spectrum (figure 4a). You can see the result in table 3.

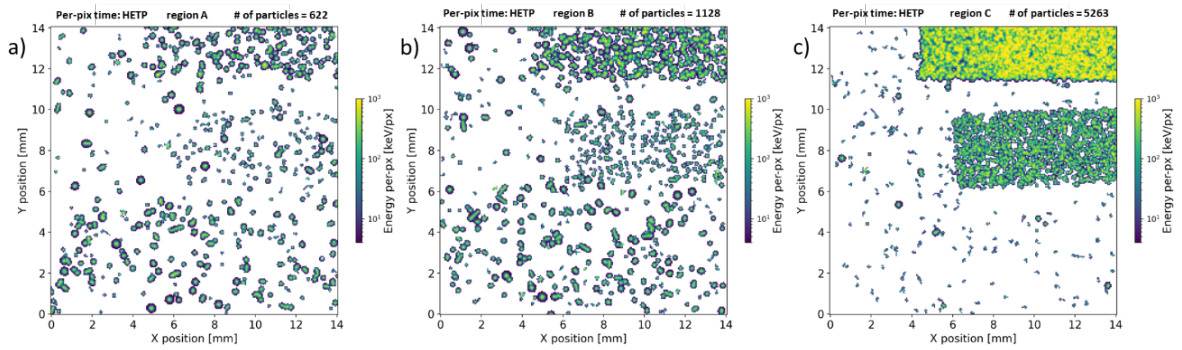

Figure 5. Time-gated spatial distributions of neutron induced events in the Timepix3 Si detector. Selective neutron-energy components: a) region "A" (see figure 4) which corresponds to the fast (14 MeV) neutron component (narrow peak in figure 4a, on left at short times 0 ms to 0.13 ms), b) Region "B" = a partly slowed-down fast component (adjacent broad peak at short times 0.13 to 0.51 ms) and c) region "C" = a broadened thermalized group (at larger times 0.51 ms to 7.74 ms). Selected events shown (HETP = class i, in table 2). The whole detector pixel-matrix is displayed = 256 × 256 px = 14 mm × 14 mm = 1.98 cm^2. The per-px energy is shown by the color bar.

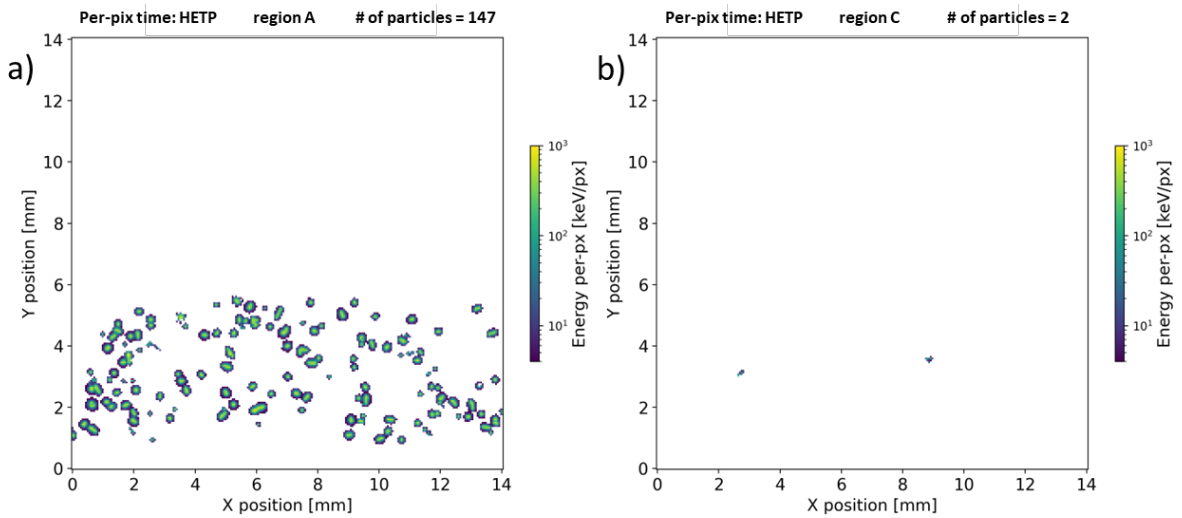

Figure 6. Similar to figure 5, showing a selected ROI spatial region a ROI time region — Visualization of PE mask based on 100 µs inteval a) the fast (14 MeV) neutron component (narrow peak on the left at short times 0 ms to 0.13 ms), b) a broadened thermalized group (at larger times 0.51 to 7.74 ms).

2025 JINST 20 C03045

Table 3. Particle-event count rates in the detector according to neutron-converter region. Values given for selected events (HETP = class i — see table 2) in the detector.

ToF region	*Flux* $[cm^{-2} \times s^{-1}]$			
	All detector area	*LiF neutron converter mask*	*Boron neutron converter mask*	*PE neutron converter mask*
A	4.41×10^{-4}	1.09×10^{-3}	6.72×10^{-4}	3.32×10^{-4}
B	7.99×10^{-4}	2.26×10^{-3}	1.51×10^{-3}	3.74×10^{-4}
C	3.73×10^{-3}	1.86×10^{-2}	7.97×10^{-3}	1.47×10^{-4}

4.4 Monte Carlo simulations

Dedicated (MC) simulation was performed using the MCNP6.2 code [11, 12] with the ENDF/B-VII.1 nuclear data library [13]. Transported particles were neutrons and photons. Particle physics options on PHYS card were kept default. The same geometry of the laboratory and the experimental setup was used in the simulation (figure 2) [14]. In the simulation the silicon surface (1 cm × 1 cm), representing the detector sensor, was irradiated by neutrons. For detailed defining of the neutron source two distributions based on the kinematics of the D-T reaction were defined of the SDEF card: a) directional neutron emission distribution and b) energy distribution of emitted neutrons in each selected solid angle bin [15]. Incoming fluxes of neutrons interacting with the silicon surface were calculated using the tally F2 for selected time (ToF) bins (T card). To achieve plausible relative errors of the total flux in the time (ToF) bins (less than 0.5%) a total of 1×10^9 particle histories were performed.

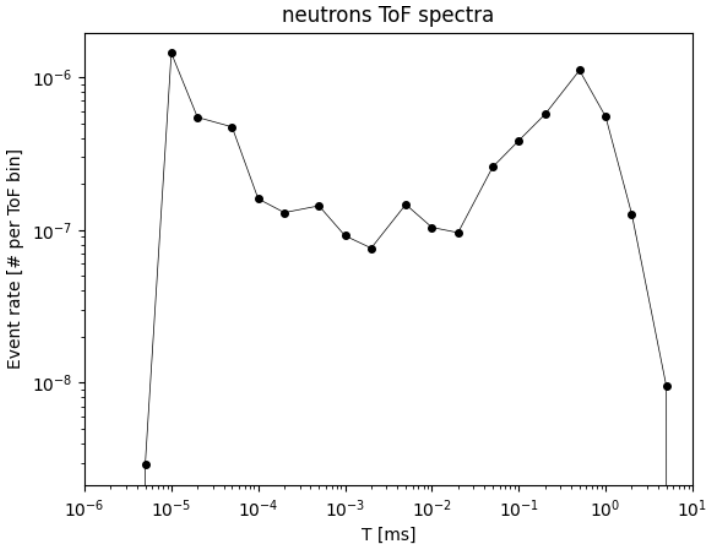

Figure 7. Neutron ToF spectrum at the detector position by Monte Carlo simulation. Values shown for the same NG settings as in the experimental section with same geometry (figure 2).

The MC simulated neutron ToF at the detector position is given in figure 7. Two components are observed. The first (left) representing incoming fast neutrons on the silicon surface and the second (right) representing thermal neutrons predominate. In the region between peaks, intermedial neutrons occur. The result of the Monte Carlo simulation corresponds to table 1 and figure 4.

2025 JINST 20 C03045

MC simulation was done to validate the experimental results and to simulate the radiation field. Also, from the MC simulation it is derived and checked that the delayed thermal neutrons arrive within one period of the operation frequency of the NG (which was 100 Hz), i.e., within 10 ms. Thanks to the comparison between the MC simulation and the experimental data, the description of the radiation field, particularly the neutron component, is more complete. The production of thermal neutrons in the delayed time interval (region C+D) is distorted by the irregularities in the pulse frequency (region D) of the NG which were observed by the detectors, see figure 4a.

The times of arrival of the neutrons to the detectors vary according to their energy (velocity) — given in table 1. This knowledge and analysis help to explain and interpret both the experimental data and the MC simulation. The fast neutron component (14 MeV) arrives within short time (<1 µs). Thermal neutrons, which are produced in the surrounding material in the laboratory walls, arrive at significantly longer times, up to several ms, before the next NG pulse — according to the MC simulation.

5 Conclusions, outlook

The Time-of-Flight (ToF) technique has been shown to be applicable using the MiniPIX Timepix3 detector, which is triggered and synchronized with a neutron generator. The pixel detector allows for the correlated spectral-, time- and position-sensitive registration of single particles with discrimination of particle-type events based on their energy, stopping power, position on the detector pixel matrix and time of arrival (ToA). The experimental and simulated ToF spectra of the D-T pulsed source used reasonably agree also with the expected exponential dependency. At the long-time low-energy region, anomalous structures in the experimental ToF spectrum can be due to distortions in the frequency repetition of the trigger signal from the NG. It is therefore necessary to verify the stability of the neutron generator. Processing of data acquired at other geometry and NG frequency-pulse settings is underway. Measurements with other pulsed sources including D-D NG and accelerator-based fast neutron sources are planned.

Acknowledgments

Preprocessing and processing of the raw data by the pixel detector were performed with DPE-TraX tool, developed in frame of Contract No. 4000130480/20/NL/GLC/hh from the European Space Agency. Work at VSB-TUO is supported by SGS project No. SP2024/016 financed by the Czech Ministry of Education, Youth and Sports.

References

[1] B. Bergmann et al., *Ionizing Energy Depositions After Fast Neutron Interactions in Silicon*, *IEEE Trans. Nucl. Sci.* **63** (2016) 2372.

[2] B. Bergmann et al., *Time-of-flight measurement of fast neutrons with Timepix detectors*, 2014 *JINST* **9** C05048.

[3] T. Czakoj et al., *The characterization of D-T neutron generators in precise neutron experiments*, *Nucl. Instrum. Meth. A* **1034** (2022) 166837.

[4] C. Granja et al., *MiniPIX Timepix3 — a miniaturized radiation camera with onboard data processing for online characterization of wide-intensity mixed-radiation fields*, 2022 *JINST* **17** C03019.

[5] C. Granja et al., *Detection of fast neutrons with the pixel detector Timepix3*, 2023 *JINST* **18** P01003.

[6] A. Novák et al., *Silicon Carbide Timepix3 detector for quantum-imaging detection and spectral tracking of charged particles in wide range of energy and field-of-view*, 2023 *JINST* **18** C11004 [arXiv:2310.17747].

[7] J. Novák et al., *New detection systems at U-120M cyclotron*, *EPJ Web Conf.* **239** (2020) 17020.

[8] M. Majerle et al., *Measurements of the neutron spectra from the p+Be neutron generator of the NPI CAS*, *Nucl. Instrum. Meth. A* **1053** (2023) 168314.

[9] A. Kruth et al., *Timepix3: a 65K channel hybrid pixel readout chip with simultaneous ToA/ToT and sparse readout*, 2014 *JINST* **9** C05013.

[10] C. Granja et al., *Resolving power of pixel detector Timepix for wide-range electron, proton and ion detection*, *Nucl. Instrum. Meth. A* **908** (2018) 60.

[11] C.J. Werner et al., *MCNP Version 6.2 Release Notes*, Los Alamos National Laboratory, Report LA-UR-18-20808 (2018) [DOI:10.2172/1419730].

[12] C.J. Werner, *MCNP User's Manual — Code Version 6.2*, Los Alamos National Laboratory, Report LA-UR-17-29981 (2017).

[13] M.B. Chadwick et al., *ENDF/B-VII.1 Nuclear Data for Science and Technology: Cross Sections, Covariances, Fission Product Yields and Decay Data*, *Nucl. Data Sheets* **112** (2011) 2887.

[14] R. Uhlář and P. Alexa, *MCNP approaches for dose rates modeling in Laboratory for neutron activation analysis and gamma spectrometry at Ostrava*, *Radiat. Prot. Dosimetry* **185** (2018) 116.

[15] R. Uhlář, P. Alexa, O. Harkut and P. Harokova, *Modified Texas Convention Method for Fast Neutron Flux Measurements*, *IEEE Trans. Nucl. Sci.* **67** (2020) 382.

2025 JINST 20 C03045